

ELECTROPHORESIS

SPECIAL ISSUE

18'08

www.electrophoresis-journal.com



CE and CEC Innovations

Editor:
Ziad El Rassi

 **WILEY-BLACKWELL**

Special Issue

CE AND CEC INNOVATIONS

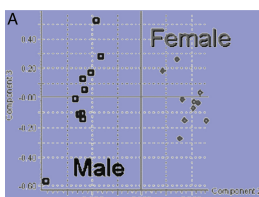
Editor: Ziad El Rassi

Editorial

3715 **CE and CEC Innovations**
Ziad El Rassi

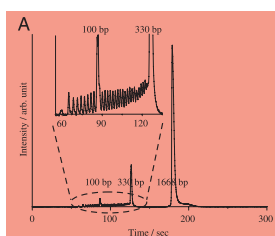
Fast Track

3717 **Development of a capillary electrophoresis-based assay of sirtuin enzymes**
Y. Fan, R. Ludewig, D. Imhof and G. K. E. Scriba



Part I: Review

3724 **Advances in separation science applied to metabonomics**
L. Xiayan and C. Legido-Quigley



Part II: Microfluidics and Miniaturization: Ion Separation, On-line Concentration and Mutation Detection

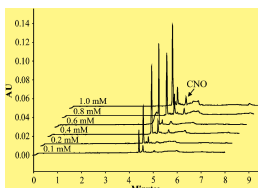
3737 **Ion separation in nanofluidics**
X. Xuan



Supporting information see www.electrophoresis-journal.com

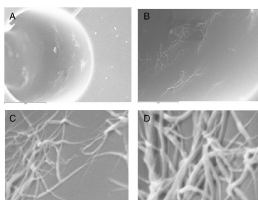
3744 **Use of a heterogeneous buffer combination in microchip electrophoresis for high-resolution separation by on-line concentration of DNA samples**
H. Nagata, M. Ishikawa, Y. Yoshida, Y. Tanaka and K. Hirano

3752 **A parylene-based dual channel micro-electrophoresis system for rapid mutation detection via heteroduplex analysis**
S. Sukas, A. E. Erson, C. Sert and H. Kulah



Part III: Novel Trends in Fundamentals and Methodologies

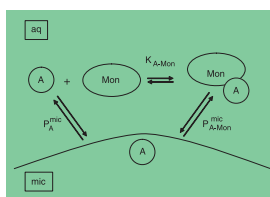
- 3759 **Evaluation of carrier ampholyte-based capillary electrophoresis for separation of peptides and peptide mimetics**
D. Koval, J.-M. Busnel, J. Hlaváček, J. Jiráček, V. Kašíčka and G. Peltre
- 3768 **Size-based characterization of nanometric cationic maghemite particles using capillary zone electrophoresis**
F. d'Orlyé, A. Varenne and P. Gareil
- 3779 **Chemometrical examination of active parameters and interactions in flow injection-capillary electrophoresis**
F. T. Dahdouh, K. Clarke, M. Salgado, G. Hanrahan and F. A. Gomez
- 3786 **Electrokinetic sample injection for high-sensitivity capillary zone electrophoresis (part 1): Effects of electrode configuration and setting**
T. Hirokawa, E. Koshimidzu and Z. Xu
- 3794 **Stacking enhanced determination of steroids by CE**
L. Bykova and L. A. Holland
-  **Supporting information see www.electrophoresis-journal.com**
- 3801 **Using multiple PCR and CE with chemiluminescence detection for simultaneous qualitative and quantitative analysis of genetically modified organism**
L. Guo, B. Qiu, Y. Chi and G. Chen
- 3810 **Enzymatic assay of marine bacterial phosphatases by capillary electrophoresis with laser-induced fluorescence detection**
K. D. Chichester, M. Sebastian, J. W. Ammerman and C. L. Colyer
- 3817 **Development of electrophoretically mediated microanalysis method for the kinetics study of flavin-containing monooxygenase in a partially filled capillary**
X. Hai, J. Konečný, M. Zeisbergerová, E. Adams, J. Hoogmartens and A. Van Schepdael



Part IV: Capillary Coatings, Open Tubular CEC, MIP-CE and Polar and Nonpolar Monoliths

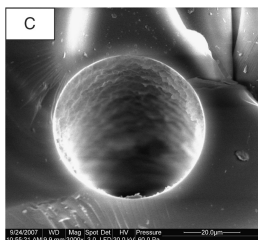
- 3825 **A novel covalent coupling method for coating of capillaries with liposomes in capillary electrophoresis**
J. Mei, J.-R. Xu, Y.-X. Xiao, X.-Y. Liao, G.-F. Qiu and Y.-Q. Feng
- 3834 **Evaluation of a molecularly imprinted polymer as in-line concentrator in capillary electrophoresis**
F. J. Lara, F. Lynen, P. Sandra, A. M. García-Campaña and F. Alés-Barrero

- 3842 **Retention of proteins and metalloproteins in open tubular capillary electrochromatography with etched chemically modified columns**
J. J. Pesek, M. T. Matyska and V. Salgotra
- 3850 **Carboxylic multi-walled carbon nanotubes as immobilized stationary phase in capillary electrochromatography**
L. Sombra, Y. Moliner-Martínez, S. Cárdenas and M. Valcárcel
- 3858 **Preparation and evaluation of butyl acrylate-based monolithic columns for CEC using ammonium peroxydisulfate as a chemical initiator**
A. Cantó-Mirapeix, J. M. Herrero-Martínez, C. Mongay-Fernández and E. F. Simó-Alfonso
- 3866 **Preparation and characterization of hexyl methacrylate monolithic columns for CEC**
A. Cantó-Mirapeix, J. M. Herrero-Martínez, C. Mongay-Fernández and E. F. Simó-Alfonso
- 3875 **CEC separation of peptides using a poly(hexyl acrylate-co-1,4-butanediol diacrylate-co-[2-(acryloyloxy)ethyl]trimethyl ammonium chloride) monolithic column**
V. Augustin, T. Stachowiak, F. Svec and J. M. J. Fréchet
- 3887 **Rapid separation and determination of microcystins using monolithic columns in isocratic elution mode by pressurized capillary electrochromatography**
C. Gu, L. Lin, B. Li, X. Chen, J. Ren, J. Jia, D. Wu and N. Fang
- 3896 **Preparation and evaluation of a lysine-bonded silica monolith as polar stationary phase for hydrophilic interaction pressurized capillary electrochromatography**
G. Huang, Q. Lian, W. Zeng and Z. Xie



Part V: MEEKC and MEKC

- 3905 **Sample stacking for the analysis of penicillins by microemulsion electrokinetic chromatography**
H.-Y. Huang and S.-H. Hsieh
- 3916 **An extended description of the effect of detergent monomers on migration in micellar electrokinetic chromatography**
A. Téllez, V. U. Weiss and E. Kenndler



Part VI: Enantioseparations by CE and CEC

- 3924 **Capillary electrophoretic chiral determination of mirtazapine and its main metabolites in human urine after enzymatic hydrolysis**
F. J. M. de Santana, V. L. Lanchote and P. S. Bonato
- 3933 **A mesoporous silica nanoparticles immobilized open-tubular capillary column with a coating of cellulose tris(3,5-dimethylphenyl-carbamate) for enantioseparation in CEC**
X. Dong, R. Wu, J. Dong, M. Wu, Y. Zhu and H. Zou
- 3941 **Chiral separation of dansyl amino acids by ligand exchange capillary electrochromatography in a low molecular weight organogel**
S. Mizrahi, D. Rizkov, A. I. Shames and O. Lev
- 3949 **Call for Papers**
- 3950 **Meetings Diary**

Access Electrophoresis from your desktop through Wiley InterScience at <http://www.electrophoresis-journal.com>.

Electrophoresis also supports EarlyView.

EarlyView is Wiley's exclusive service presenting individual articles online as soon as they are ready, even before the release of the compiled print issue. EarlyView articles are complete, peer-reviewed, and citable. Speak to your librarian or visit the site for full details.



For the USA and Canada:

Electrophoresis (ISSN 0173-0835) is published bi-weekly by Wiley-VCH, PO Box 191161, 69451 Weinheim, Germany. Air freight and mailing in the USA by Publications Expediting

Inc., 200 Meacham Ave., Elmont NY 11003. Periodicals postage paid at Jamaica, NY 11431. US POST-MASTER: send address changes to *Electrophoresis*, Wiley-VCH, 111 River Street, Hoboken, NJ 07030,

Annual subscription price for institutions: US\$ 4722/4292 (valid for print and electronic/print or electronic delivery). Postage and handling charges included. All prices are subject to local VAT/sales tax.

Xiangchun Xuan

Department of Mechanical Engineering, Clemson University, Clemson, SC, USA

Received February 7, 2008

Revised March 24, 2008

Accepted April 14, 2008

Research Article**Ion separation in nanofluidics**

Ionic species with a constant charge-to-size ratio (*i.e.* electrophoretic mobility) cannot be separated in electroosmotic or pressure-driven flow along microscale channels. In nanoscale channels, however, the enormous electric fields inside electrical double layers cause transverse ion distributions yielding charge-dependent mean ion speeds in the flow. Those ions with a constant charge-to-size ratio can thus be separated solely by charge (or equivalently, size) in nanofluidics. Here we develop an analytical model to optimize and compare the separation of such ions in nanochannel chromatography and nanochannel electrophoresis in terms of selectivity, plate height and resolution. Both planar and cylindrical geometries are considered. It is found that in nanoscale channels chromatography yields a larger selectivity and a larger minimum reduced plate height than electrophoresis does. The maximum resolution is, however, comparable between these two nanofluidic approaches, where the optimal channel half-height or tube radius is within the range of 1–10 times the Debye length. Our results also suggest that cations can be better separated in nanofluidics than can anions.

Keywords:Ion separation / Nanochannel chromatography / Nanochannel electrophoresis / Nanofluidics / Resolution
DOI 10.1002/elps.200800098**1 Introduction**

CE is a routine analytical technique that uses electric fields to separate ionic species with different electrophoretic mobilities or charge-to-size ratios in a micro capillary or a micro-fabricated channel. Chromatography is another family of separation techniques for species varying in interaction with a stationary phase that may be packed or coated onto a micro-column. These species are passed through the stationary phase in a pressure-driven or electric field-driven mobile phase. However, neither electroosmotic flow nor pressure-driven flow is able to separate ions with a constant charge-to-size ratio in free solutions through microchannels. This issue may be resolved by nanofluidics, *viz.* fluid flow in nanochannels, which has been growing exponentially over the past decade [1–5]. In nanoscale channels where the hydraulic diameter is comparable to the electrical double layer (EDL) thickness, the enormous electric fields inside EDL produce transverse ion distributions that depend on the ion charge [6–10]. As a consequence, the non-uniform fluid

flow along nanochannels, which may be electric field-driven [11, 12] or pressure-driven [11–14], yields charge-dependent mean ion speeds enabling the separation of ions by charge alone.

The ion separation in electroosmotic flow along nanoscale channels, *i.e.* nanochannel electrophoresis, was first proposed and implemented by Pennathur and Santiago [11] and Garcia *et al.* [12]. Following them, Griffiths and Nilson [13], and Xuan and Li [14] proposed to separate ions in pressure-driven flow along nanoscale channels, named here as nanochannel chromatography (note: not a strict definition). Both groups theoretically compared the ion separation in these two nanofluidics-based technologies in terms of retention (*i.e.* ratio of the mean speed of ionic species to that of neutral species). The ion dispersion in nanofluidics has also been analyzed and compared in between chromatography and electrophoresis [13, 15–18]. However, both retention and dispersion are associated with only one type of ions, and provide no direct measure of the separation between two types of ions. The objective of this paper is to optimize and compare the separation of ions with a constant charge-to-size ratio in nanochannel chromatography and nanochannel electrophoresis in terms of selectivity, plate height and resolution. Nanoscale planar channels and round tubes will both be considered in the analytical model. For the separation of ions with different electrophoretic mobilities in nanofluidic channels, which may be the result of dissimilar ion charges or dissimilar ion diffusivities, readers are referred to [13, 14].

Correspondence: Professor Xiangchun Xuan, Department of Mechanical Engineering, Clemson University, Clemson, SC, USA
E-mail: xcxuan@clemson.edu
Fax: +1-864-656-7299

Abbreviation: EDL, electrical double layer

2 Theory

2.1 Ion transport in nanofluidics

The local ion speed, u_i , in a combined pressure-driven and electroosmotic flow along a straight, uniform channel is given by

$$u_i = u_p + u_e + v_i z_i F E \quad (1)$$

where u_p is the pressure-driven fluid velocity, u_e the electroosmotic fluid velocity, v_i the ion mobility, z_i the ion charge, F the Faraday's constant and E the axial electric field either externally applied in electroosmotic flow or internally induced in pressure-driven flow (*i.e.* so-called streaming potential field) [19]. Note that the product, $v_i z_i F$, is the ion electrophoretic mobility referred to in Section 1, and will be assumed constant in Section 3. The two fluid velocity components are expressed as [20–22]

$$u_p = \frac{a^2}{2^{n+1}\mu} \left(1 - \frac{y^2}{a^2}\right) P \quad \text{and} \quad u_e = -\frac{\epsilon\zeta}{\mu} \left(1 - \frac{\Psi}{\zeta^*}\right) E \quad (2)$$

where a is the half-height of a planar channel ($n = 0$) or the radius of a round tube ($n = 1$), μ the fluid viscosity, y the transverse coordinate originating from the channel axis, P the pressure drop per unit channel length, ϵ the fluid permittivity and $\zeta^* = F\zeta/RT$ the dimensionless form of the wall zeta potential ζ with R the universal gas constant and T the absolute fluid temperature.

The non-dimensional EDL potential in Eq (2), $\Psi = F\psi/RT$, is solved from the Poisson–Boltzmann equation [23]

$$\frac{1}{y^n} \frac{d}{dy} \left(y^n \frac{d\Psi}{dy} \right) = \kappa^2 \sinh(\Psi) \quad (3)$$

where $\kappa = \sqrt{2F^2 c_b / \epsilon RT}$ is the inverse of the so-called Debye screening length with c_b being the ionic concentration of a symmetric, unit-charge electrolyte (*e.g.* KCl). Here again, $n = 0$ indicates a planar channel while $n = 1$ indicates a round tube. It is recognized that the applicability of Eq. (3) to nanoscale channels might be questionable especially to those with strong EDL overlapping [24, 25]. However, Eq. (3) has been successfully used to explain the experimentally measured electrical conductance and streaming current in variable nanofluidic channels [26–30]. For the case of a small ζ^* which is desirable for sensitive ion separations in nanochannels as demonstrated by Griffiths and Nilson [13], one may use the Debye–Huckel approximation in Eq. (3), that is $\sinh(\Psi) = \Psi$, yielding [31]

$$\Psi = \zeta^* \frac{\cosh(\kappa y)}{\cosh(\kappa a)} \quad (4)$$

in a channel ($n = 0$) and

$$\Psi = \zeta^* \frac{I_0(\kappa y)}{I_0(\kappa a)} \quad (5)$$

in a tube ($n = 1$), where I_0 denotes the zero order modified Bessel function of the first kind, and κa can be viewed as the normalized channel half-height or tube radius.

As a consequence of the transverse ion distributions produced by the electric fields inside EDLs, the mean ion speed (zone velocity) \bar{u}_i in nanofluidics becomes dependent on the ion charge z_i and is given by [7–18]

$$\bar{u}_i = \bar{u}_{ip} + \bar{u}_{ie} + v_i z_i F E \quad (6)$$

$$\bar{u}_{ip} = \frac{\langle u_p B_i \rangle}{\langle B_i \rangle} \quad \text{and} \quad \bar{u}_{ie} = \frac{\langle u_e B_i \rangle}{\langle B_i \rangle} \quad (7)$$

where \bar{u}_{ip} and \bar{u}_{ie} denote, respectively, the mean ion speed due to pressure-driven fluid flow and electroosmotic fluid flow, $\langle \dots \rangle = (n+1) \int_0^a (\dots) (y/a)^n dy/a$ signifies the cross-sectional area-average ($n = 0$ or 1) and $B_i = \exp(-z_i \Psi)$ characterizes the Boltzmann distribution of ions in the transverse direction. In nanochannel electrophoresis, no pressure gradient is applied so that $\bar{u}_{ip} = 0$. In nanochannel chromatography, downstream accumulation of counter-ions results in the development of a streaming potential field [19–23]. This induced electric field E_{st} can be determined from the zero current condition through the channel, as presented below.

The electric current density j in a combined pressure-driven and electroosmotic nanochannel flow is given by [16–23, 32]

$$j = -\frac{1}{y^n} \frac{d}{dy} \left(y^n \frac{d\Psi}{dy} \right) \frac{\epsilon RT}{F} (u_p + u_e) + c_b \lambda_b \cosh(\Psi) E \quad (8)$$

where λ_b is the molar conductivity of the bulk electrolyte. In this equation the surface conductance of the outer diffusion layer in the EDL has been considered through the cosine hyperbolic function [21, 22]. The contribution of the inner Stern layer conductance [23, 33, 34] to the electric current is, however, ignored. Substituting u_p and u_e with Eq. (2) and then area-averaging the new Eq. (8) lead to

$$E_{st} = \frac{g_1 / \zeta^*}{2^n c_b F (g_2 + \beta g_3 / \zeta^{*2})} P \quad (9)$$

where in a channel ($n = 0$)

$$g_1 = 1 - \frac{\tanh(\kappa a)}{\kappa a}, \quad g_2 = \frac{\tanh(\kappa a)}{\kappa a} - \frac{1}{\cosh^2(\kappa a)}$$

and

$$g_3 = \int_0^a \cosh(\Psi) d\left(\frac{y}{a}\right) \quad (10)$$

and in a tube ($n = 1$)

$$g_1 = 1 - \frac{2I_1(\kappa a)}{\kappa a I_0(\kappa a)}, \quad g_2 = \frac{I_1^2(\kappa a)}{I_0^2(\kappa a)} + \frac{2I_1(\kappa a)}{\kappa a I_0(\kappa a)} - 1$$

and

$$g_3 = \int_0^a \cosh(\Psi) \left(\frac{y}{a}\right) d\left(\frac{y}{a}\right) \quad (11)$$

In Eq. (9), $\beta = \lambda_b \mu / \epsilon RT$, whose reciprocal was termed Levine number by Griffiths and Nilson [32], is a non-dimensional product of fluid properties, and spans only the range $2 < \beta < 10$ for normal aqueous solutions [33].

2.2 Ion separation in nanofluidics

Separation performance in chromatography and electrophoresis is typically characterized by selectivity, plate height (or plate number, *i.e.* efficiency) and resolution [35]. Selectivity, r_{ji} , is defined as the ratio of the mean speeds of ions i and j

$$r_{ji} = \bar{u}_i / \bar{u}_j \quad (12)$$

and should be larger than 1 as traditionally defined. A larger r_{ji} indicates a better separation.

Plate height, H_i , is the spatial variance of the ion peak distribution, σ_i^2 , divided by the migration distance, L , within a time period of t_i . High separation efficiency in chromatography and electrophoresis requires a small H_i , which is often expressed in the following dimensionless form of a reduced plate height, h_i [35]

$$h_i = \frac{H_i}{a} = \frac{\sigma_i^2}{aL} = \frac{2D'_i t_i}{aL} = \frac{2D'_i}{a\bar{u}_i} \quad (13)$$

where D'_i is the effective diffusion coefficient due to a combination of hydrodynamic dispersion and molecular diffusion. All other sources of dispersion such as injection and detection, refer to [36, 37] for detail, have been neglected here. According to the Taylor–Aris dispersion theory [38, 39], the effective diffusion coefficient is given by [39, 40]

$$D'_i = D_i(1 + \chi_i Pe_i^2) \quad (14)$$

where D_i is the ion diffusivity and $Pe_i = \bar{u}_i a / D_i$ is the Peclet number based on the mean ion speed. The dispersion coefficient, χ_i , is determined from [35, 41]

$$\chi_i = \left\langle B_i^{-1} \left[y^{-n} \int_0^y B_i(u_i / \bar{u}_i - 1) y^n dy \right]^2 \right\rangle \langle B_i \rangle^{-1} \quad (15)$$

Note that χ_i is not a function of the driving force [*i.e.* E in electrophoresis or P in chromatography, see Eq. (2)] and the ion Peclet number as well.

Following Griffiths and Nilson's analysis [13], we combine Eqs. (13) and (14) to rewrite the reduced plate height as

$$h_i = 2(1/Pe_i + \chi_i Pe_i) \quad (16)$$

Therefore, h_i attains its minimum

$$h_{i,\min} = 4\sqrt{\chi_i} \text{ at } Pe_{i,\text{opt}} = 1/\sqrt{\chi_i} \quad (17)$$

In other words, there exists an optimal value for the mean ion speed, $\bar{u}_{i,\text{opt}} = D_i/a\sqrt{\chi_i}$, and thus an optimal electric field in nanochannel electrophoresis or an optimal pressure gradient in nanochannel chromatography, at which the separation efficiency is maximized. An identical formula to Eq. (17) has been obtained for $h_{i,\min}$ in the paper by Griffiths and Nilson [13]. There are, however, two aspects pertinent to the present dispersion coefficient that have been neglected in Griffiths and Nilson's analysis. One is the ion electrophoretic mobility in nanochannel electrophoresis, and the other is the flow-induced streaming potential field (and thus fluid electroosmosis and ion electrophoresis) in nanochannel chromatography. These two aspects may bring

substantial influences on both the selectivity (actually retention in previous papers) and the plate height [13, 14, 16–18].

Resolution, R_{ji} , can be defined in two different ways: the one introduced by Giddings [42], Eq. (18), and the one adopted by Huber [43] and Kenndler [44–46], Eq. (19),

$$R_{ji} = \frac{t_j - t_i}{2(\sigma_{t,i} + \sigma_{t,j})} \quad (18)$$

$$R_{ji} = \frac{t_j - t_i}{\sigma_{t,i}} \quad (19)$$

where t is the migration time as defined in Eq. (13) and σ_t is the standard deviation of ion peak distribution in the time domain. In either of these two definitions, a larger value of R_{ji} indicates a better separation. For simplicity, Eq. (19) is used here to calculate the resolution. Hence, substituting $t_i = L/\bar{u}_i$, $t_j = L/\bar{u}_j$ and $\sigma_{t,i} = \sigma_i/\bar{u}_i$ into Eq. (19) gives

$$R_{ji} = \frac{L}{\sigma_i} (r_{ji} - 1) = \frac{\sqrt{L/a}}{\sqrt{h_i}} (r_{ji} - 1) \quad (20)$$

Referring back to Eq. (17), it is straightforward to obtain

$$R_{ji,\max} = \frac{\sqrt{L/a}}{\sqrt{h_{i,\min}}} (r_{ji} - 1) \text{ at } Pe_{i,\text{opt}} = 1/\sqrt{\chi_i} \quad (21)$$

because the selectivity r_{ji} is independent of the ion Peclet number as alluded to above.

3 Results and discussion

A MATLAB program was written to compare the performance of ion separation in nanochannel chromatography and nanochannel electrophoresis by examining the selectivity, r_{ji} in Eq. (12), minimum reduced plate height, $h_{i,\min}$ in Eq. (17), and maximum resolution, R_{ji} in Eq. (21). We focus on the separation of ions with a constant electrophoretic mobility, *i.e.* $v_i z_i F$ in Eq. (1), which is equivalent to a constant charge-to-size ratio or a constant product, Dz , of the ion charge and diffusivity because the ion size is inversely proportional to its diffusivity *via* the Nernst–Einstein equation [23, 33]. These ions are unable to be separated in either pressure-driven or electroosmotic microchannel flows.

A typical value of the ion charge–diffusivity product, $Dz = 10^{-10} \text{ m}^2/\text{s}$, was selected in the calculations while the ion charge was varied from -4 to $+4$. The non-dimensional zeta potential was fixed to $\zeta^* = -2$ corresponding to a zeta potential value of about -50 mV , at which the use of linear approximation in Eq. (3) is still valid as demonstrated previously [8, 21, 31]. The ionic concentration of the electrolyte (*e.g.* KCl aqueous solution) was chosen as $c_b = 1 \text{ mM}$, and the Levine number was $\beta = 4$, which is typical for aqueous solutions [32, 33]. The ratio of channel length to channel half-height or tube radius was assumed to be $L/a = 10^4$ for convenience. We recognize that fixing the channel length might be a wiser option when the channel height or tube radius is varied. Presented below are only the

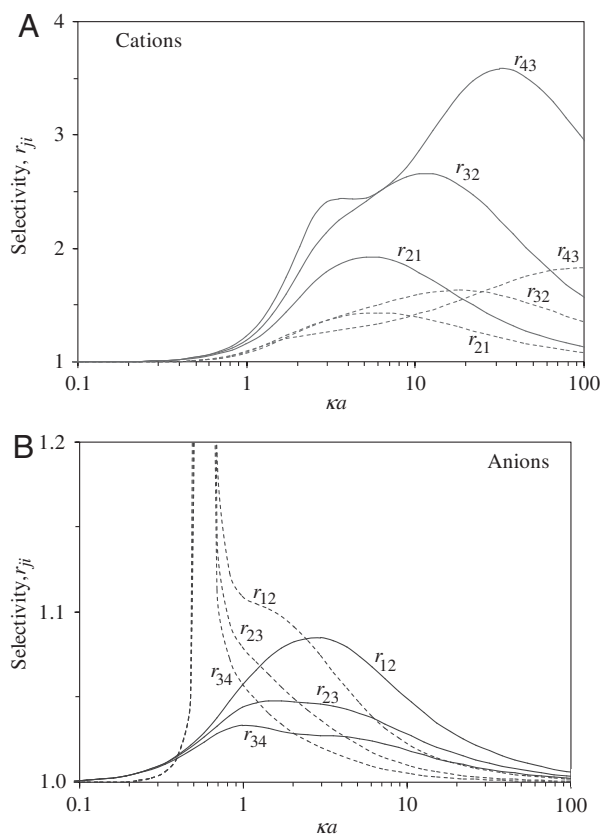


Figure 1. Selectivity, r_{ji} , of (A) cations and (B) anions in nanochannel chromatography (solid lines) and nanochannel electrophoresis (dashed lines).

results for the nanoscale planar channels. Those for nanoscale round tubes are quantitatively very similar and thus all moved to the Supporting Information.

Figure 1 compares the selectivity, r_{ji} , of (A) cations and (B) anions in nanochannel chromatography (solid lines) and nanochannel electrophoresis (dashed lines). It is important to note that the indices of r_{ji} , which indicate the charge values of the two ions to be separated (For instance: r_{21} for cations indicates the selectivity between positive ions of charges +1 and +2, and r_{12} for anions indicates the selectivity between negative ions of charges -1 and -2), are switched between cations and anions in order that $r_{ji} > 1$ as traditional defined [35]. Specifically, we use r_{21} , r_{32} , and r_{43} for cations (or more generally, ions with $z_i z_j^* < 0$) as those with higher charges are concentrated in a region of smaller fluid speed (*i.e.* closer to the channel wall) and thus move slower. In contrast, anions (or ions with $z_i z_j^* > 0$) with higher charges appear predominantly in the region of larger fluid speed (closer to the channel center) and thus move faster. Therefore, we need to use r_{12} , r_{23} and r_{34} for anions. This index switch also applies to the resolution, R_{ji} , to be illustrated in Fig. 3.

One can see in Fig. 1A that the selectivity, r_{ji} , of cations in nanochannel chromatography is always greater than that

of the same pair of cations in nanochannel electrophoresis. This discrepancy gets larger when the ion charge number increases. Meanwhile, the optimal κa value at which r_{ji} is maximized increases for both chromatography and electrophoresis though it is always smaller in the former case. The discrepancy between these two optimal κa also increases with the rise of ion charge. For example, r_{21} in nanochannel chromatography reaches the maximum 1.93 at $\kappa a \approx 5$ while in electrophoresis r_{21} is at most 1.45 when $\kappa a \approx 6$. As a comparison, the maximum r_{43} in chromatography is 3.59 at $\kappa a \approx 31$ while in electrophoresis it becomes 1.85 at $\kappa a \approx 100$. The last two values of κa actually correspond to sub-micron channels where there exists a very weak EDL overlapping. However, the still relative large $z_i z_j^*$ (-6 for $z_i = +3$ ion and -8 for $z_i = +4$ ion) is sufficient to provide a high sensitivity of separation. This result agrees with Griffiths and Nilson's [13] analysis of charged ion retention.

For anions, Fig. 1B shows a significantly lower r_{ji} than for cations in nanochannel chromatography. Moreover, r_{ji} decreases when the ion charge number increases. The optimal κa at which r_{ji} is maximized is also smaller than that for cations, and decreases (but only slightly) with the ion charge. For example, the maximum $r_{12} = 1.09$ appears at $\kappa a \approx 2.5$, indicating that the best separation of anions in chromatography occurs only in nanoscale channels with a strong EDL overlapping. All these results apply equally to r_{ji} of anions in nanochannel electrophoresis except at around $\kappa a = 0.6$ where r_{ji} varies rapidly with κa and goes higher than 2. Within this region of κa , the electrophoretic velocity of anions is close to the fluid electroosmotic velocity [more accurately, \bar{u}_{ie} in Eq. (6)] while in the opposite direction. Therefore, the net ion speed is essentially so small that even a trivial difference in the ion speed (essentially the difference in \bar{u}_{ie} as the ion electrophoretic velocity is constant due to the fixed charge-to-size ratio of ions) could yield a large r_{ji} .

It is, however, important to note that a reversal of anion speed (*i.e.* anions migrate to the anode side instead of the cathode side along with the electrolyte solution) could take place in nanochannel electrophoresis when κa is less than a threshold value (*e.g.* $\kappa a = 0.6$ in Fig. 1B). In such circumstances, it is likely that only one of the two anionic species migrates toward the detector no matter the detector is placed in the cathode or the anode side of the channel. Another consequence is that the maximum r_{ji} in nanochannel electrophoresis might be achieved with a fairly long analysis time, which makes the separation practically meaningless. We therefore expect that ions with a constant electrophoretic mobility can be better separated in nanochannel chromatography than in nanochannel electrophoresis. Moreover, cations (or more generally, ions with $z_i z_j^* < 0$) can be separated more easily than can anions (or ions with $z_i z_j^* > 0$).

Figure 2 displays the minimum reduced plate height, $h_{i,\min}$, of (A) cations and (B) anions in nanochannel chromatography (solid lines) and nanochannel electrophoresis (dashed lines). For a clearer comparison, $h_{0,\min}$ of neutral species in both methods are also included in the plots. As noted in Section 2, $h_{i,\min}$ in Eq. (17) is essentially different

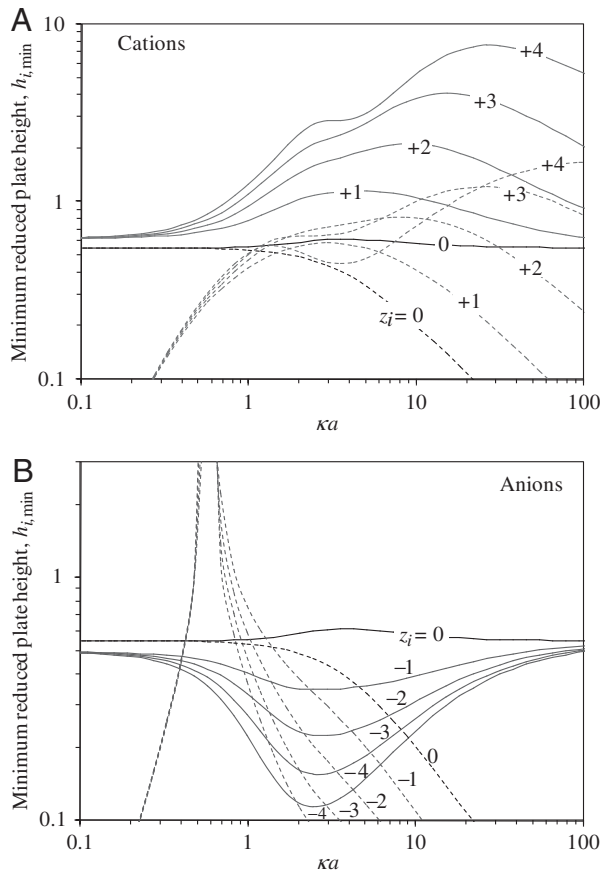


Figure 2. Minimum reduced plate height, $h_{i,min}$, of (A) cations and (B) anions in nanochannel chromatography (solid lines) and nanochannel electrophoresis (dashed lines).

from that derived by Griffiths and Nilson [13] though they possess exactly the same form. We therefore do not intend to compare Figure 2 with their results. It is, however, noted that $h_{0,min}$ (or the dispersion coefficient χ_0) agrees very well with Griffith and Nilson's results for electrophoresis [13] and Xuan and Sinton's results [16] for chromatography.

As shown in Figure 2A, $h_{i,min}$ of cations in nanochannel chromatography (solid lines) is roughly an order of magnitude larger than that in electrophoresis (dashed lines) except at very small or very large κa , indicating a higher separation efficiency in electrophoresis. In chromatography, $h_{i,min}$ of cations is larger than $h_{0,min}$, and increases with the charge number z_i . In electrophoresis, however, $h_{i,min}$ exhibits a relatively complicated dependence on z_i . Both $h_{i,min}$ have a relative large value for an intermediate channel size, $1 < \kappa a < 100$. For large κa , the EDL thickness is so thin that the ion distribution becomes uniform across the channel. Therefore, the hydrodynamic dispersion in electrophoresis (or the so-called electrokinetic dispersion [47]) reduces with κa [48, 49] and so does $h_{i,min}$. In this same limit, the flow-induced streaming potential is negligible as $g_2 \rightarrow \infty$ [see Eqs. (9)–(11)]. Hence, $h_{i,min}$ in chromatography should approach

$4\sqrt{2/105} = 0.552$ where the value inside the square root is the dispersion coefficient of neutral species for pure pressure-driven flow in a planar channel [39, 50]. For small κa , $h_{i,min}$ of cations in nanochannel chromatography approaches 0.623 though the EDL potential is uniform across the channel and so is the ion distribution. This last value is dependent on the ion charge–diffusivity product, Dz , as defined above. In the same limit, $h_{i,min}$ of cations in nanochannel electrophoresis becomes independent of the ion charge and approaches zero because of the constant while finite Dz .

In contrast to cations, $h_{i,min}$ of anions in nanochannel chromatography (solid lines in Fig. 2B) is smaller than $h_{0,min}$ of neutral species and decreases when the magnitude of ion charge z_i increases (*i.e.* from -1 to -4). Moreover, $h_{i,min}$ of anions varies with κa in an opposite way to that of cations (solid lines in Fig. 2A). These results also apply to $h_{i,min}$ of anions in nanochannel electrophoresis unless κa is small. Therefore, anions yield higher separation efficiency than do cations, which is contrary to the selectivity, r_{ji} , where cations are actually preferred in both chromatography and electrophoresis. In addition, $h_{i,min}$ of anions in chromatography approaches 0.496 when κa is very small while converging to 0.552 when κa is very large due to the reasons stated above. In electrophoresis, $h_{i,min}$ decreases with κa when $\kappa a > 1$. At about $\kappa a = 0.6$, there occurs a sharp rise in $h_{i,min}$ due to the small magnitude of the net ion speed around this κa value. This variation is consistent with that of r_{ji} in Fig. 1B. In the low limit of κa , $h_{i,min}$ of anions in electrophoresis becomes again independent of the ion charge and approaches zero. Overall, $h_{i,min}$ is on the order of 1, indicating that submicrometer or even nanometer plates heights are attainable for channel dimensions of the order of 100 nm. However, as Griffiths and Nilson [13] have pointed out recently, the injection and detection volumes must then be extremely small to realize the full capability of these nanofluidics-based ion separation techniques.

Figure 3 compares the maximum resolution, $R_{j,max}$, of cations and anions (as labeled) in nanochannel chromatography (solid lines) and nanochannel electrophoresis (dashed lines). The indices of $R_{j,max}$ are assigned following those of the selectivity, r_{ji} , in Figure 1, to ensure $R_{j,max} > 0$. One can see that $R_{j,max}$ of cations in chromatography is larger than that of anions throughout the range of κa . In electrophoresis, cations also yield a better resolution than anions do if $\kappa a > 1$. When $\kappa a < 1$, $R_{j,max}$ of anions increases and reaches the extremes at $\kappa a = 0.6$ due to the sudden rise in both the selectivity (refer to Fig. 1B) and the reduced plate height (refer to Fig. 2B) as described above. Within the same range of κa , $R_{j,max}$ of cations continues decreasing when κa decreases and thus becomes smaller than that of anions. Interestingly, chromatography and electrophoresis offer a comparable resolution for both cations and anions in nanoscale channels if $\kappa a > 1$. This result may release previous concerns [13, 14] that nanochannel electrophoresis might be problematic in separating ions by charge due to the effects of ion electrophoresis.

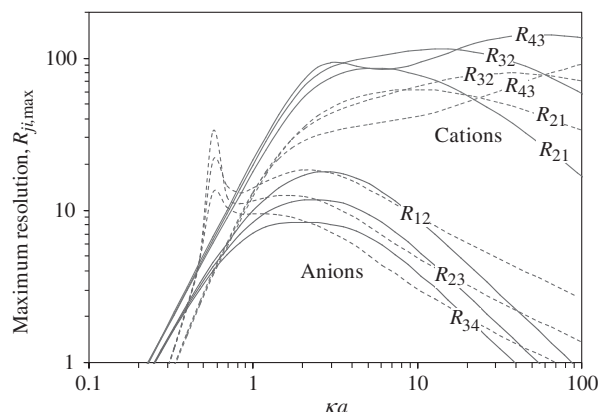


Figure 3. Maximum resolution, $R_{ji,max}$, of cations and anions in nanochannel chromatography (solid lines) and nanochannel electrophoresis (dashed lines).

It is also noted in Figure 3 that the optimal channel size for both separation methods appears to be $1 < \kappa a < 10$. In other words, the best channel half-height (and tube radius as well, see the Supporting Information) for ion separation in nanofluidics will be $10 \text{ nm} < a < 100 \text{ nm}$ when 1 mM electrolyte solutions are used. In this context, the optimum Peclet number to achieve the maximum resolution in a channel of $\kappa a = 5$ (or $a \approx 50 \text{ nm}$) will be $Pe_{i,opt} = O(4)$ because $h_{i,min} = O(1)$ as noted above [see also Eqs. (17) and (21)]. Although this Peclet number (corresponding to the mean ion speed of the order of 8 mm/s) seems a little too high in current nanofluidics, it indicates that large fluid flows are preferred in both nanochannel chromatography and nanochannel electrophoresis for high throughputs and separation efficiencies.

4 Conclusions

We have derived closed formulae for the selectivity, plate height and resolution to optimize and compare the ion separation in nanochannel chromatography and nanochannel electrophoresis. Ions with a constant charge-to-size ratio are selected to demonstrate the advantage of these nanofluidic approaches over the traditional CE and chromatography in microscale channels. Results show that nanochannel chromatography offers a larger selectivity and a larger minimum reduced plate height than nanochannel electrophoresis does. The maximum resolution in which selectivity and plate height play competing roles is thus comparable between these two nanofluidics-based separations. The optimal channel half-height or tube radius to achieve the maximum resolution for all ions seems to be within the range of 1–10 times the Debye length. This size (e.g. $10 \text{ nm} < a < 100 \text{ nm}$ in 1 mM electrolyte solutions) is readily available with the current nano-fabrication facility [51]. Our results also suggest that cations can be better separated in nanofluidics than can anions though the resolution of anions might reach a higher

level in smaller nanochannels at the cost of longer analysis times.

Financial support from Clemson University through a start-up package to X.X. is gratefully acknowledged.

The authors have declared no conflict of interest.

5 References

- [1] Eijkel, J. C. T., van den Berg, A., *Microfluid. Nanofluid.* 2005, 1, 249–267.
- [2] Mijatovic, D., Eijkel, J. C. T., van den Berg, A., *Lab. Chip.* 2005, 5, 492–500.
- [3] Yuan, Z., Garcia, A. L., Lopez, G. P., Petsev, D. N., *Electrophoresis* 2007, 28, 595–610.
- [4] Holtzel, A., Tallarek, U., *J. Sep. Sci.* 2007, 30, 1398–1419.
- [5] Han, J., Fu, J., Schoch, R., *Lab Chip* 2008, 8, 23–33.
- [6] Pennathur, S., Santiago, J. G., *Anal. Chem.* 2005, 77, 6772–6781.
- [7] Petsev, D. N., *J. Chem. Phys.* 2005, 123, 244907.
- [8] Xuan, X., Li, D., *Electrophoresis* 2006, 27, 5020–5031.
- [9] Dutta, D., *J. Colloid. Interf. Sci.* 2007, 315, 740–746.
- [10] Dutta, D., *Electrophoresis* 2007, 28, 4552–4560.
- [11] Pennathur, S., Santiago, J. G., *Anal. Chem.* 2005, 77, 6782–6789.
- [12] Garcia, A. L., Ista, L. K., Petsev, D. N., O'Brien, M. J. *et al.*, *Lab Chip* 2005, 5, 1271–1276.
- [13] Griffiths, S. K., Nilson, R. N., *Anal. Chem.* 2006, 78, 8134–8141.
- [14] Xuan, X., Li, D., *Electrophoresis* 2007, 28, 627–634.
- [15] De Leebeeck, A., Sinton, D., *Electrophoresis* 2006, 27, 4999–5008.
- [16] Xuan, X., Sinton, D., *Microfluid. Nanofluid.* 2007, 3, 723–728.
- [17] Xuan, X., *Anal. Chem.* 2007, 79, 7928–7932.
- [18] Xuan, X., *J. Chromatography A* 2008, 1187, 289–292.
- [19] Li, D., *Colloid. Surf. A* 2001, 191, 35–57.
- [20] Burgreen, D., Nakache, F. R., *J. Phys. Chem.* 1964, 68, 1084–1091.
- [21] Rice, C. L., Whitehead, R., *J. Phys. Chem.* 1965, 69, 4017–4024.
- [22] Hildreth, D., *J. Phys. Chem.* 1970, 74, 2006–2015.
- [23] Hunter, R. J., *Zeta Potential in Colloid Science, Principles and Applications.* Academic Press, New York 1981.
- [24] Qu, W., Li, D., *J. Colloid Interface Sci.* 2000, 224, 397–407.
- [25] Taylor, J., Ren, C. L., *Microfluid. Nanofluid.* 2005, 1, 356–363.
- [26] Stein, D., Kruithof, M., Dekker, C., *Phys. Rev. Lett.* 2004, 93, 035901.
- [27] Karnik, R., Fan, R., Yue, M., Li, D. *et al.*, *Nano Lett.* 2005, 5, 943–948.

- [28] Fan, R., Yue, M., Karnik, R., Majumdar, A., Yang, P., *Phys. Rev. Lett.* 2005, 95, 086607 (1–4).
- [29] Van der Heyden, F. H. J., Stein, D., Dekker, C., *Phys. Rev. Lett.* 2005, 95, 116104.
- [30] Van Der Hayden, F. H. J., Bonthuis, D. J., Stein, D., Meyer, C., Dekker, C., *Nano Lett.* 2007, 7, 1022–1025.
- [31] Li, D., *Electrokinetics in Microfluidics*. Elsevier Academic Press, Burlington, MA 2004.
- [32] Griffiths, S. K., Nilson, R. H., *Electrophoresis* 2005, 26, 351–361.
- [33] Probstein, R. F., *Physicochemical Hydrodynamics*. Wiley, New York 1995.
- [34] Davidson, C., Xuan, X., *Electrophoresis* 2008, 29, 1125–1130.
- [35] Giddings, J. C., *Unified Separation Science*. Wiley, New York 1991.
- [36] Gas, B., Stedry, M., Kenndler, E., *Electrophoresis* 1997, 18, 2123–2133.
- [37] Gas, B., Kenndler, E., *Electrophoresis* 2000, 21, 3888–3897.
- [38] Taylor, G. I., *Proc. Roy. Soc. London A* 1953, 219, 186–203.
- [39] Aris R. *Proc. Roy. Soc. London A* 1956, 235, 67–77.
- [40] Dutta, D., Ramachandran, A., Leighton, D. T., *Microfluid. Nanofluid.* 2006, 2, 275–290.
- [41] Martin, M., Giddings, J. C., *J. Phys. Chem.* 1981, 85, 727–733.
- [42] Giddings, J. C., *Sep. Sci.* 1969, 4, 181–189.
- [43] Huber, J. F. K., *Fresenius' Z., Anal. Chem.* 1975, 277, 341–347.
- [44] Kenndler, E., *J Capillary Elec.* 1996, 3, 191–198.
- [45] Schwer, C., Kenndler, E., *Chromatographia* 1992, 33, 331–335.
- [46] Kenndler, E., Fridel, W., *J Chromatography* 1992, 608, 161–170.
- [47] Ghosal, S., *Annu. Rev. Fluid Mech.* 2006, 38, 309–338.
- [48] Griffiths, S. K., Nilson, R. H., *Anal. Chem.* 1999, 71, 5522–5529.
- [49] Griffiths, S. K., Nilson, R. N., *Anal. Chem.* 2000, 72, 4767–4777.
- [50] Wooding, R. A., *J. Fluid. Mech.* 1960, 7, 501–515.
- [51] Perry, J. L., Kandikar, S. G., *Microfluid. Nanofluid.* 2006, 2, 185–193.